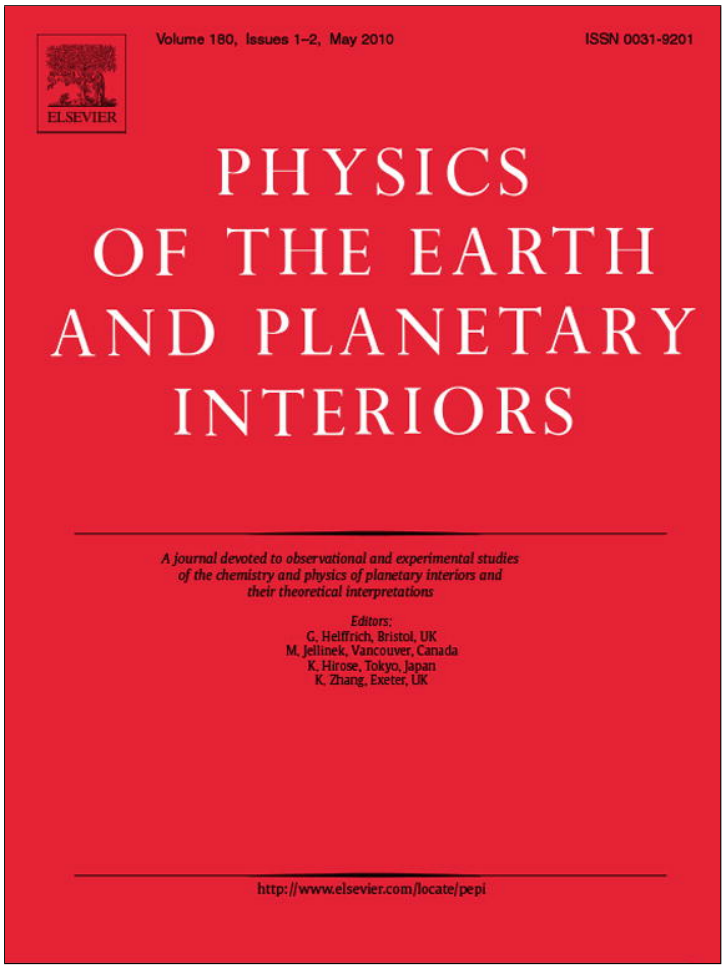

Physics of the Earth and Planetary Interiors 180 (2010) 41–51

Contents lists available at ScienceDirect

Physics of the Earth and Planetary Interiors

journal homepage: www.elsevier.com/locate/pepi

Absolute geomagnetic intensity data from preclassic Guatemalan pottery

L.M. Alva-Valdivia[a,*], J. Morales[b], A. Goguitchaichvili[b], M. Popenoe de Hatch[c], M.S. Hernandez-Bernal[d,e], F. Mariano-Matías[a,b,c,d,e]

[a] Laboratorio de Paleomagnetismo, Instituto de Geofisica, Universidad Nacional Autónoma de México, Ciudad Universitaria, 04510 México D.F., Mexico
[b] Laboratorio Interinstitucional de Magnetismo Natural, Instituto de Geofísica, Unidad Michoacán, Universidad Nacional Autónoma de México, Campus Morelia, Mexico
[c] Departamento de Arqueología de la Universidad del Valle de Guatemala, Guatemala
[d] Instituto de Geologia, Universidad Nacional Autónoma de México, Ciudad Universitaria, 04510 México D.F., Mexico
[e] Universidad Michoacana de San Nicolas de Hidalgo, Morelia, Michoacán, Mexico

ARTICLE INFO

Article history:
Received 27 March 2009
Received in revised form 2 March 2010
Accepted 5 March 2010

Keywords:
Archaeointensity
Magnetic properties
Mesoamerica
Guatemala
Preclassic pottery

ABSTRACT

Archaeointensity results from 10 pottery fragments from the Kaminaljuyu area (14°37′N, 90°32′W)—Guatemala, whose ages range from 100 to 900 B.C., were determined in order to contribute to the incipient intensity secular variation curve for the preclassic period in Mesoamerica. Magnetic experiments including hysteresis loops, IRM-DIRM and Curie temperature analysis indicate that pseudo-single-domain magnetite and/or titanium poor titanomagnetites are responsible for the remanence. Pottery fragments were analyzed using the Coe version of the Thellier and Thellier paleointensity method. Although not numerous, our results meet with high standard, commonly accepted strict selection and acceptance criteria as attested by reasonably high Coe quality factors. The fragment mean archaeointensities range from 15 to 43 μT, and corresponding virtual axial dipole moments range from 3.6 ± 0.7 to $10.3 \pm 0.9 \times 10^{22}$ Am^2. This corresponds to a mean VADM value of $(7.5 \pm 2.5) \times 10^{22}$ Am^2, which is close to the present day field strength. The new results obtained in this study together with those of *ArcheoInt* data compilation, are analyzed in context of CALS3k and ARCH3K model predictions.

1. Introduction

After Nagata's and Bucha's pioneering works in Mesoamerica in the 1960s (Nagata et al., 1965; Bucha et al., 1970) a gap in archaeomagnetic studies in the region seems to have opened (Rodriguez-Ceja et al., 2009; Morales et al., 2009). Archaeomagnetic and particularly archaeointensity data are still sparse and of variable quality in spite of the abundant, well controlled archaeological vestiges available in the region. Main limitation of archaeomagnetic studies is the fact that most of burned archaeological artifacts are displaced and thus no primary geomagnetic directions may be retrieved. However, archaeointensity studies have the great advantage that no oriented material is required.

On the other hand, rapid development of archaeointensity determinations occurred in Europe which allows the use of geomagnetic field intensity fluctuations as a dating tool (Genevey and Gallet, 2002). Archaeomagnetic dating consists of comparing magnetic parameters (direction and/or intensity) of an archaeological artifact against a known record of geomagnetic variation in order to associate a date to the archaeological piece under study (Aitken, 1990). The precision of any archaeomagnetic date obtained will therefore depend upon the precision of the calibration curve itself, and on the way in which the comparison is made.

The main purpose of the present investigation is to contribute new reliable data to the incipient archaeointensity reference curve for Mesoamerica. Ten pottery fragments from the Kaminaljuyu area (14°37′N, 90°32′W) (Fig. 1), with ages ranging from 100 to 900 B.C., were used to accomplish this task. Thellier–Coe method was employed for the intensity determinations. Raw intensity data were cooling rate corrected and a mean VADM value of $(7.5 \pm 2.5) \times 10^{22}$ Am^2, close to the present day field strength was obtained. Present data, together with those of ArcheoInt data compilation (Genevey et al., 2008) were compared in context of CALS3k and ARCH3K model predictions.

2. Pottery/sample description

The sherds subjected to analysis in this report came mainly from the archaeological site of Kaminaljuyu, the largest and most important center in the Central Highlands of Guatemala during the Preclassic period (800 B.C.–200 A.D.). Strategically located on the Continental Divide where the trade routes connecting the Pacific coast, the Atlantic coast and the highlands to the north and north-

* Corresponding author. Tel.: +52 55 56224237; fax: +52 55 55509395.
E-mail addresses: lalva@geofisica.unam.mx, labrax54@yahoo.com.mx (L.M. Alva-Valdivia).

0031-9201/$ – see front matter © 2010 Elsevier B.V. All rights reserved.
doi:10.1016/j.pepi.2010.03.002

west intersect, it became the hub of a large commercial network where goods from distant areas were exchanged and transported between highlands and lowlands. At its height it consisted of over 200 major structures distributed over an area of some 5 km^2. A major cultural shift occurred around 150 A.D. when the site was taken over by an intrusive population which remained in control until the site was finally abandoned around 800 A.D. (Popenoe de Hatch, 1997).

Today most of the site of Kaminaljuyu is buried under the urban constructions of modern Guatemala City. The archaeological information from the site has been obtained from excavations carried out in recent decades and the analysis of the ceramics from the site. The presence of Maya-style sculpture and a few instances of hieroglyphic writing have suggested to epigraphers and linguists that Kaminaljuyu was probably inhabited by Maya, probably Cholan, speakers. The site was first occupied by these groups who arrived with full knowledge of construction techniques, agricultural techniques and some hydraulic technology for simple irrigation, and advanced skills for making pottery and knapping obsidian tools. The region from where they came to settle in the valley of Guatemala is not known, but the evidence suggests it may have been somewhere in the region of the Pacific South Coast of Guatemala or even El Salvador. The motivation for resettlement seems to have been the interest in setting up the long-distance trade network.

2.1. Steps in pottery manufacture

The sherds utilized in the present analysis are mostly from Kaminaljuyu, with a few from the Pacific and Atlantic watersheds included for comparative purposes (Table 1). The sherds from these areas were probably made in pottery-making centers close to each of the sites. Ethnographic studies of native pottery manufacture, which apparently are survivals of Precolumbian traditions, give an idea of how the craft was carried out. The wheel for this purpose was not known, but in some cases the lump of clay was set on a plate in front of the potter and spun around as she (or he) built up the wall of the vessel. In other cases a concave or convex mold might have been used to form the body of the vessel, the rim, handles, and decoration then added by hand. Less commonly the potter, a woman in the cases observed, was the wheel, placing the lump of clay on the ground and then running around it as she gradually pulled up the clay to form the wall. The rim and base are added to complete the vessel, handles and supports as necessary, and in the final steps applying modeled or incised decoration.

After the pot has dried (which usually takes a day or two in the open air), a slip can be applied. The slip is a solution of very fine clay particles or paste which is applied over the vessel and then burnished using a smooth stone to give a bright polish. The slip and polish seal the pores to render the surface impermeable, and often give an attractive color according to the minerals which are present or added to the clay. Painted decoration can be applied over the slip.

Some instances of earthen kilns for firing clay have been observed ethnographically but most frequently the vessels are baked in an open fire. In this process the vessels, after being thoroughly dried, are piled up one over the other cushioned with twigs and pine needles, topped with more fine branches and then fired. The preferred wood for the firing is oak, although pine and other trees can also serve when oak is not available. Temperatures are probably well below 900 °C with a lower bound of 500 °C (Sinipoli, 1991: 29–30). An hour or so after the start of firing, the first vessels are removed using long poles to lift them out, and the potters then rearrange the remaining ones which are not quite ready for removal, adjusting them to the heat to complete their firing. Temperatures never reached the sufficient heat to permit vitrification (or glazing) in Precolumbian times until very late in the Late Classic period. At this time, around 700 A.D. one ware (called Plumbate Ware) was developed on the South Coast which is the only case of true vitrified pottery clay from Mesoamerica. Whether the necessary temperature was reached in a kiln or in an open fire is not known.

2.2. Sherd provenence and dates

Ceramics are usually dated according to styles (a combination of form, technology and decoration) which vary chronologically and according to local preferences. The dating of ceramic styles, however, is related to materials associated with the sherds or vessels which permit absolute dating, either by geochemical methods based on unstable isotopes such as C14, or archaeomagnetic techniques, thermoluminescence, obsidian hydration, etc. In the Classic Maya Lowlands, dates can be derived from those inscribed on associated hieroglyphic texts.

In the current analysis, seven of the ten sherds were obtained from two archaeological projects at the ancient site of Kaminaljuyu, one carried out in 1983 (Popenoe de Hatch, 1997) and the other in 1995 (Popenoe de Hatch, 2000). These sherds were probably all manufactured in the vicinity of the site. The 1983 project recovered the sherd D-304h at approximately 2.5 m depth in the fill of a large irrigation canal discovered during the season. The canal measured at its maximum 18 m in width and at least 6 m in depth and was designed to drain water from an ancient lake to irrigate what were probably vegetable crops cultivated in raised garden plots. The irrigation system dates from around 700 B.C. to 100 A.D. when there is evidence that the lake waters dried up, probably due to a number of factors including over-exploitation of the waters, cutting of the surrounding forests, and/or tectonic movements. The final phases of use of the canal (dated by the ceramics in the fill) show that it was silting at the end of Late Preclassic period, around 100 A.D. Subsequently, the canal was completely filled in and small residences were built on the surface.

The sherd 254/4d was also recovered during the 1983 excavations at Kaminaljuyu. It was found with many others in what had been an earth oven in a large area devoted to food preparation, presumably a communal kitchen, near the area where crops were cultivated and watered by the canal irrigation. The earth oven was oval in form, reaching 150 cm at its maximum diameter, tapering to a narrower width at the base at a depth of 340 cm. This part of the kitchen area with its oven and an associated hearth was probably roofed with thatch or palm leaves. The roofed area covered approximately 11 m × 15 m. Eventually the oven fell into disuse, the roof apparently collapsed and the area was left to the elements allowing it to be silted in with rain-deposited sediments. From the fill of the oven were recovered abundant sherds mixed with burned earth and ashes. The levels from 100 to 340 cm date to Late Preclassic times (ca. 300 B.C. to 100 A.D.). Above this the fill contained a few Early Classic sherds, but after this the oven ceased to be used.

The large kitchen area, which seems to have functioned for cooking in very large quantities, continued to in use during the Early Classic period (150–450 A.D.). The sherd D-275/2b came from the fill of one of five earth ovens found in this area, all associated with grinding stones, clay griddles, a few whole vessels, and abundant sherds mixed with ash and lumps of burned clay. The sides of this oven were nearly vertical and the base was flat; its maximum diameter measured 1.50 m and it reached a depth of 1.0 m. The analysis of carbonized residues in one of the ovens included charred seeds of avocados, jocotes, beans, zapotes and anonas. The large number of burned avocado seeds (high in oil content) in the ovens suggests they were employed as live coals to assist in long, slow baking of food.

The sherd D-275-8b was found in an Early Classic trash pit of irregular form which contained pottery fragments, parts of obsidian cores and flakes, along with burned clay lumps. Surprisingly, it had

Fig. 1. Location map of the the Kaminaljuyu area, southern part of Guatemala.

been re-used for an informal, probably secondary, burial. The burial was evidenced by very scattered human teeth and a few bits of bone.

The sherd labeled A-P-G-Sy was recovered from one of three successive trash pits encountered in the 1970s during repairs of a highway along the outskirts of Guatemala City. The contents of the pits were donated to the Kaminaljuyu archaeological project carried out in 1983 where the sherds could be studied. It was determined that they pertain to the Late Preclassic period and consisted almost entirely of large jars which, for various reasons, are considered to have been used for storage of cacao. Because of their portability and high demand for consumption, cacao beans were used as a medium of exchange in Precolumbian Mesoamerica. The trash pits were subsequently found to be part of a much larger zone where many more pits with similar storage jars had been discarded. It has been argued that the zone functioned as a type of "bank" where cacao had been stored for use by the Kaminaljuyu governing body for use in its function as the large trade center in the highland region during Preclassic times. The sherd in question came from one of the large, broken jars.

In 1995 the second archaeological project was initiated at Kaminaljuyu which had as its objective the recovery of more information regarding the canal irrigation system. Sherds KJM-161-3 and 161-8 were recovered from one of several very large trash pits discovered and excavated during this project. The trash pits could be dated to the transition between the Late Preclassic and Early Classic periods, when an intrusive group usurped the governing power at Kaminaljuyu. The KJM-161 pit, located in a residential mound, reflects the gradual absorption of the Early Classic styles into the older Preclassic ceramic complex, according to the technological fashions imposed by the new ruling group.

The rest of the sherds subjected to analysis in this report come from regions quite distant from the central highlands of Guatemala. The sherd K-60A was collected from the surface of the Pacific Coast of Guatemala near the Mexican border, in an area fairly close to the shore of the Pacific Ocean where the early occupants (around 1200–900 B.C.) were exploiting the estuary and riverine resources and preparing salt for export (Coe and Flannery, 1967). The population using ceramic types in this particular complex was probably not a maya group; it has been argued that they belonged to the Mixe-Zoque language group (Lowe, 1977). The styles of the ceramics suggest local manufacture according to stylistic norms that were commonly shared in the region of Chiapas, Mexico.

In the region not far distant from the above, sherd K-62h was recovered from excavations at the site of La Blanca on the South Coast of Guatemala, along the edge of the Rio Naranjo near the

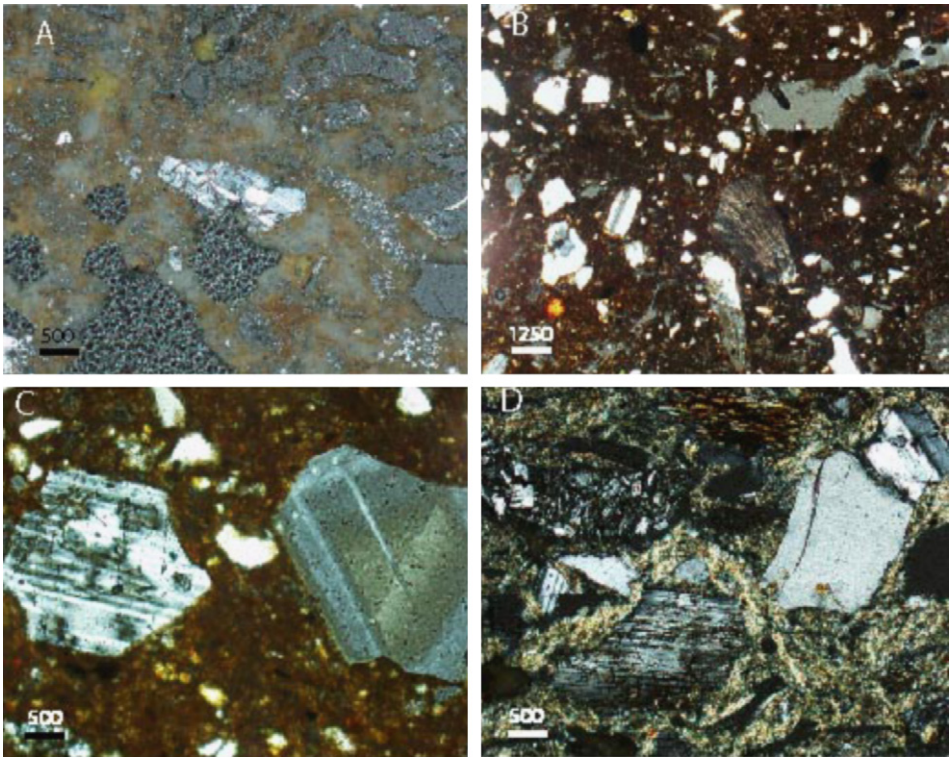

Fig. 2. Microphotographs of transparent minerals of representative samples. Scale bar is in microns. (A) From Sample 4, shows at the centre a subhedral oligoclase crystal embedded in a vitreous matrix partly devitrified to clayish minerals. Also are observed several vitreous fragments; (B) (Sample 6) shows a general field with an anhedral quartz crystal close to the centre and a subhedral plagioclase plus several vitreous fragments all embedded in a vitreous matrix; Sample 4 (C) shows a broken spherulite fragment of orthoclase, through all the sample there are fractures occupied by colloidal silica. Finally, (D) (Sample 7) shows a subhedral crystal of plagioclase (center-down) with anomalous anisotropy and an anhedral quartz crystal embedded in a vitreous matrix partly devitrified. All is partly altered to clayish and sericite minerals.

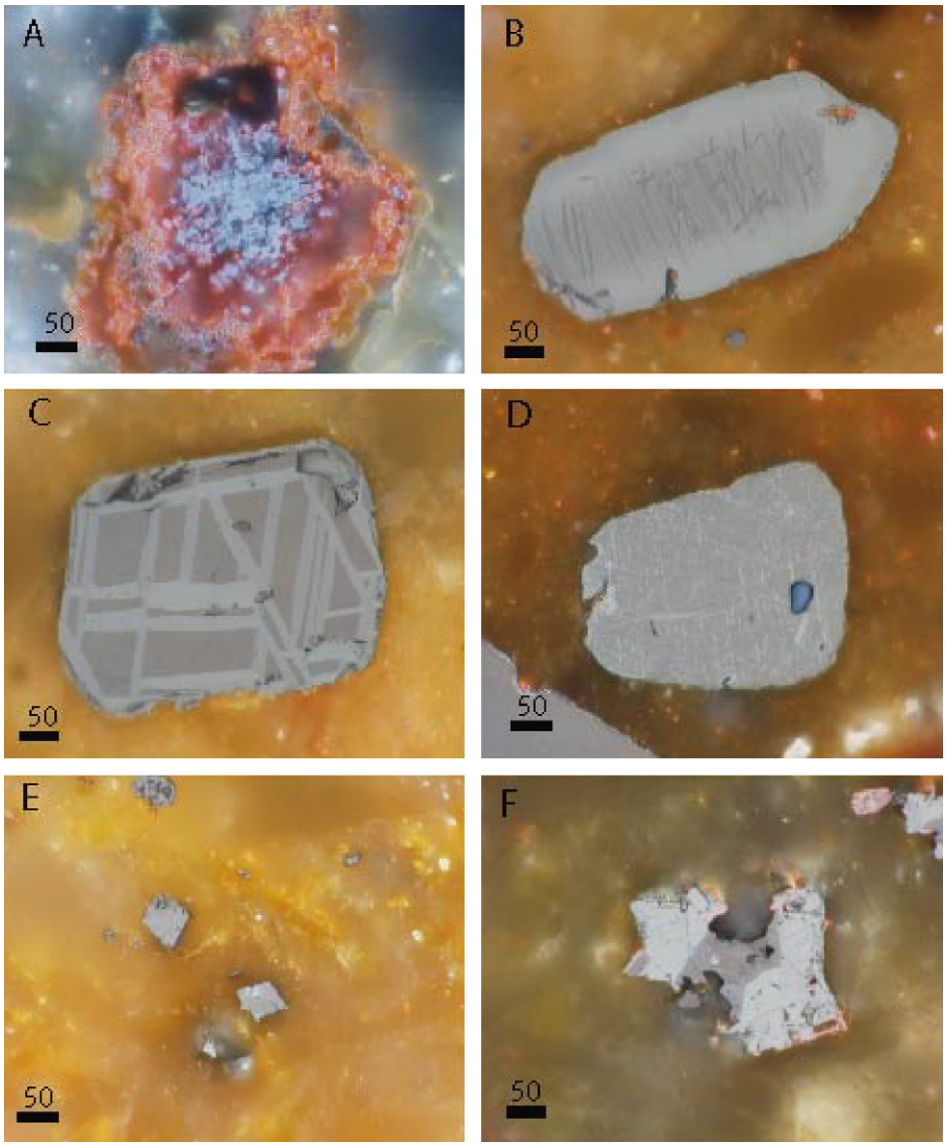

Fig. 3. Microphotographs of opaque minerals of representative samples. Scale bar is in microns. (A) (Sample 6) shows a titanohematite grain of skeletal texture altered to limonite; Sample 4 shows in (B) a titanomagnetite octahedral crystal partly altered to titanomaghemite, showing at the centre acicular ilmenite lamellae and holes filled with rutile; (C) (Sample 4) shows an octahedral titanomagnetite crystal with ilmenite and titanohematite lamellae; pseudomorphous titanohematite crystal with ilmenite lamellae in trellis texture and pseudobrookite and rutile as product of alteration, (D) (Sample 8); Sample 1 (E) shows two titanomagnetite octahedral crystals, partly altered to titanomaghemite and titanohematite. Lastly, (F) (Sample 3) shows a titanomagnetite grain, skeletal texture, altered to titanohematite with ilmenite lamellae partly altered to rutile along its borders.

Mexican border. The ceramics show that the site was occupied by people (possibly also of the Mixe-Zoque language group) related to the Olmec culture in Mexico. The esoteric nature of the styles and forms of the ceramics and the large number of figurines gives the impression that the site was mainly ceremonial in its function. The ceramics were not widely traded and were probably of local manufacture and use. The ceramics also indicated that the site was occupied by high status individuals, the dates of their occupation ranging from around 800 to 600 B.C.

The final sherd, E-42g, comes from a surface collection at the site of Tulumaje Viejo, El Progreso, on the Atlantic watershed of Guatemala. The site was occupied during Middle and Late Preclassic times (ca. 800–100 B.C.) but the style of the sherd places it fairly early in the period. Tulumaje Viejo had a close association with Kaminaljuyu, probably through trade in obsidian and jade which had their sources in the lower Motagua river valley, not far from Tulumaje Viejo. The sherd represents the most characteristic and abundant type in the region.

These ten sherds should provide a representative sample of Preclassic ceramics from Kaminaljuyu in the highlands of Guatemala, with contrasting examples from both the Atlantic and Pacific sides of the Continental Divide.

3. Microscopic observations under transmitted/reflected light

Optical examination of 10 thin polished sections, corresponding to studied pottery fragment, allows the estimation of petrography (Fig. 2) and opaque minerals (Fig. 3) concentration subdivided into fractions of titanomagnetite, titanohematite, and titanomaghemite. We followed Buddington and Lindsley (1964) in classifying textures and Haggerty (1976) in resolving oxidation states. The main results can be summarized as follows.

Titanomagnetites are transformed to Ti-poor titanomagnetite. Titanomagnetites show anhedral to subhedral texture with

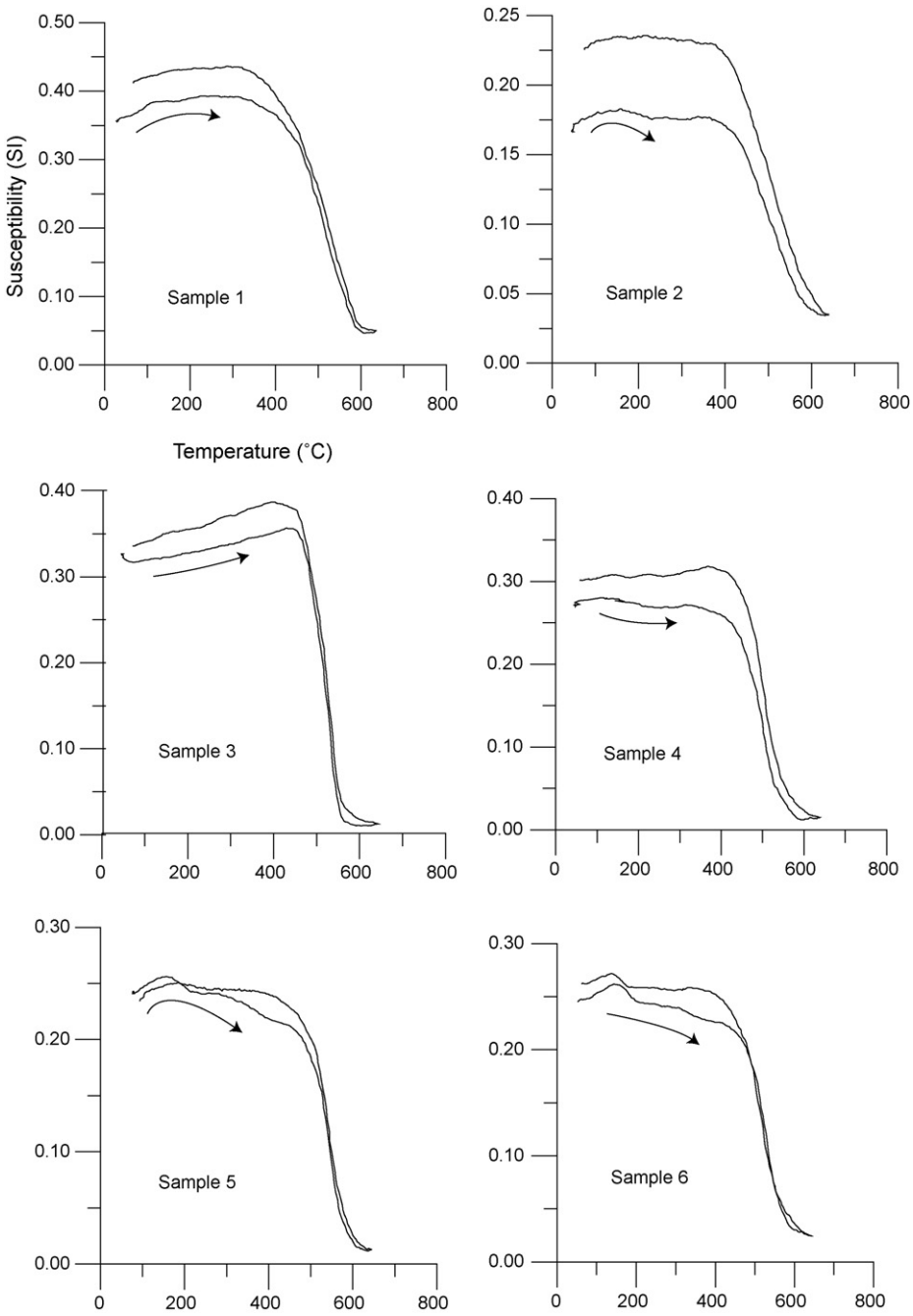

Fig. 4. Continuous low-field high temperature susceptibility curves (in air) of representative samples. Arrows indicate heating curves. Cooling curves suggest small phase changes possible of titanomaghemite to magnetite.

ilmenite lamellas. There is just few (titano)maghemite, and hematite is scarce. Titanomagnetite seems to be the main magnetic carrier in studied rocks. However, it is not homogeneous with ilmenite intergrowths showing a light gray-brown color, sometimes fractured or with a brecciated texture. The general characteristics of magnetic mineralogy show deuteric oxidation of degree C1 and C2 (Haggerty, 1976) and a possible light hydrothermal alteration.

These observations under microscope suggest that Ti-poor titanomagnetite (almost magnetite) is the dominant magnetic carrier. Although few titanohematites and titanomagnetites are observed, their contributions in remanent magnetization should be minor. Here, we would like to underline the importance of the microscopy study to estimate the origin the remanence. As showed by Draeger et al. (2006), there are no proved magnetic tests to distinguish between thermoremenent and chemical remanence while the microscopic observation under reflected light is probably the unique way to discriminate between primary (TRM) and secondary (CRM) magnetizations. The titanomagnetite-ilmenite intergrowth of trellis or sandwich form is the principal feature of the studied samples. This texture type is commonly developed during deuteric oxidation which occurs at temperatures higher than Curie points of main magnetic carriers. Thus, the magnetization measured is thermoremanent origin.

3.1. Alteration degree

The alteration degrees (1–3) are a function of the alteration degree of the matrix, limonite abundance and alteration degree of

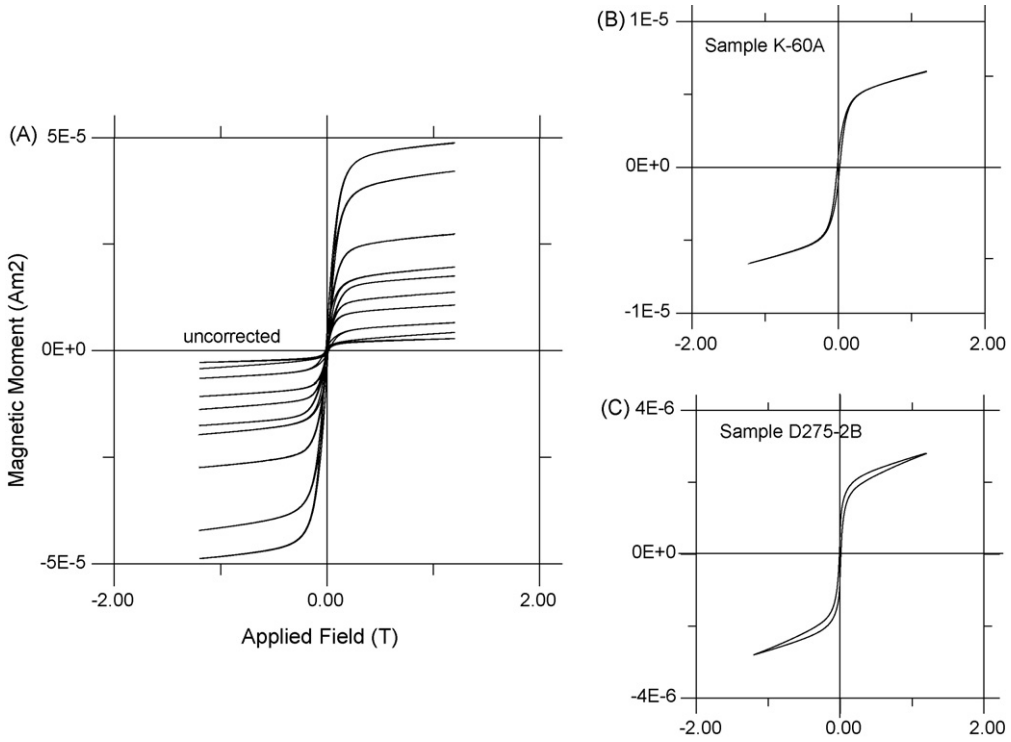

Fig. 5. Hysteresis plots. Coercivity is very small, generally (K-60A), and slight predominance is of pseudo-single-domain behavior probably due to the very fine grain size of the clay from which the potteries are made. Wasp-waisted behavior is detected in sample D275-2B.

the mineral crystal and volcanic rock fragments embedded in the matrix.

Alteration degree 1, samples 2 and 6 (Fig. 2B) is represented by crystal fragments showing angular to subangular borders of Na plagioclase (oligoclase and andesine), orthoclase, quartz, and ferromagnesian (mica) minerals, as well as scarce volcanic fragments. All is embedded in a vitreous matrix partly altered to clay and sericite with a minor proportion of Fe oxides of granular texture disseminated homogeneously. Fe oxides correspond to titanomagnetite slightly altered to titanomaghemite and to titanohematite, and scarce proportion of limonite. The altered titanomagnetite shows ilmenite lamellas and is partly altered to pseudobrookite and to rutile.

Alteration degree 2, samples 7 and 9 (Fig. 2D) is represented by fresh angular fragments of quartz and Na plagioclase, as well as orthoclase fragments slightly altered to sericite and clayish minerals. Angular fragments of volcanic rocks are in minor proportion, as well as Na plagioclase and ferromagnesian (mica and hornblende) which show Fe oxides (titanohematite and limonite) filling fractures. All the fragments are embedded in a vitreous matrix extremely altered to sericite and clayish minerals associated to Fe oxides homogeneously disseminated. Fe oxides are titanomagnetite with ilmenite lamellas, both occasionally altered to titanohematite and pseudobrookite, respectively. This alteration degree 2, shows higher matrix alteration than alteration degree 1, as well as limonite filling the open spaces in the minerals.

Alteration degree 3, samples 1, 3, 4, 5, 8 and 10 (Fig. 2A) is represented by fresh angular fragments of quartz and Na plagioclase, as well as orthoclase fragments altered to sericite and clayish minerals. Ferromagnesian fragments (biotite, hornblende and some pyroxenes, diopside) show a light alteration patina. Fragments of volcanic rocks are in major proportion, with Fe oxides (hematite and limonite) filling open spaces and fractures in some Na plagioclase. All fragments are embedded in a sericite, clay and limonite matrix (being the characteristic of this alteration number). Fe oxides are fresh or altered titanomagnetite with ilmenite lamellas, both occasionally altered to titanohematite–pseudobrookite, and rutile. These minerals are embedded in the volcanic rock fragments and a few in the matrix.

4. Rock-magnetic experiments

Magnetic characteristics of typical samples are summarized in Figs. 4–6 and are described as follows:

1. Continuous low-field susceptibility vs. high temperature curves (Fig. 4) shows, in most cases, the presence of a single ferri-

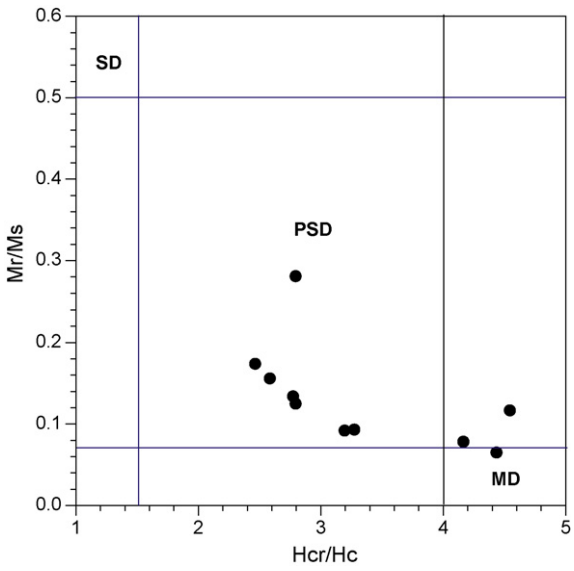

Fig. 6. Room temperature hysteresis parameters plotted as a Day plot (see text for more details).

Table 1
List of ceramic samples and their relative chronology in regional context.

Area	Sample	Provenence	Age
Costa Sur	1 (K-60A)	Salinas La Blanca, surface collection	~900 B.C.
Costa Sur	7 (K-62h)	La Blanca, surface collection	~800 B.C.
Baja Verapaz	2 (E42g)	Tulumaje Viejo, El Progreso, barranca	~500 B.C.
Kaminaljuyu	3 (KJM-3B-161-3)	Excavation Project Miraflores, 60 cm	~400 B.C.
Kaminaljuyu	6 (D-275-2b)	Excavation Project San Jorge, 40 cm	~200 B.C.
Kaminaljuyu	10 (D-275-8b)	Excavation, Project San Jorge, 160 cm	~200 B.C.
Kaminaljuyu	5 (D-304h)	Excavation Project San Jorge, 160 cm	200–100 B.C.
Kaminaljuyu	4 (A-P-G-Sy)	Excavation Trash Pit, Highway San Juan	~100 B.C.
Kaminaljuyu	8 (D-254/4d)	Excavation, Project San Jorge, 80 cm	~100 B.C.
Kaminaljuyu	9 (KJM-3B-161-8)	Excavation, Project Miraflores, 160 cm	~100 B.C.

magnetic phase with Curie point compatible with nearly pure magnetite. However, the cooling and heating curves are occasionally not perfectly reversible (cooling curves slightly higher than heating curves indicating transformation during the heating in air).

2. Hysteresis measurements at room temperature were performed on all studied samples using the AGFM 'Micromag' apparatus of the paleomagnetic laboratory at Mexico City in fields up to 1.4 T (Fig. 5). The curves are symmetrical in all cases. Near the origin, no potbellied and wasp-waisted behavior (Tauxe et al., 1996) was detected, which probably reflect very restricted ranges of the opaque mineral coercivities. The only exception is Sample 6, which probably reflects the presence of ferrimagnetic phases with different coercivities. Most probably this behavior is due to the presence of dominantly single-domain and superparamagnetic grains. For other samples (Fig. 5a and b), 'small' pseudo-single-domain grains seem to be responsible for remanence, judging from hysteresis parameters values (Day et al., 1977; Fig. 6). This probably indicates a mixture of multidomain and a significant amount of single-domain (SD) grains. Let us note that if some superparamagnetic fraction exists also in these samples, the measured coercive force and saturation magnetization are somewhat lower or larger, respectively, than those ferrimagnetic fractions alone. Generally speaking, estimation of the domain state and/or mineralogical composition of archaeological samples by means of hysteresis parameters seems to be more difficult than in rocks or synthetic samples (e.g., Aitken et al., 1991; Chauvin et al., 2000; Genevey and Gallet, 2002; Morales et al., 2009). This is basically due to the nature of the raw material (mud/clay) used for manufacturing archaeological artifacts.

5. Sample preparation and archaeointensity determinations

Individual archaeomagnetic mini-cores were 'packed' into salt (NaCl) pellets in order to treat them as standard paleomagnetic cores. Magnetization per unit volume of 'blank' pellets ranges on the order of 10^{-5} A/m, whereas magnetization of typical archaeomagnetic mini-cores selected for PI determinations ranges on the order of 10^{-2} to 10^{-1} A/m. Measurements of remanences were carried out using a JR6 spinner magnetometer. Archaeointensity (AI) experiments were performed following the method developed by Thellier and Thellier (1959) as modified by Coe (1967). Following the paleodirectional and rock-magnetic results, altogether 69 samples belonging to each of the 10 pottery fragments, yielding stable, one component magnetization with blocking temperatures compatible to near magnetite phase and with relatively high median destructive field (MDF) values were selected for AI experiments. Heatings and coolings were accomplished in air using a thermal demagnetizer (MMTD80). The experiments were carried out in two stages: first stage consisted of a set of 10 pilot samples (i.e., 1 sample per fragment), 11 temperature steps were distributed between room temperature and 565 °C and the laboratory field set to 40 μT. Second stage comprises a set of 59 samples; here only 8 temperature steps were applied since their unblocking temperature spectra were already well identified and the laboratory field was reset to 30 μT. pTRM's checks every 2 steps were distributed through the whole temperature spectrum during the AI experiments in both stages.

5.1. Cooling rate and ATRM correction procedures

Cooling rate (CR) dependence of TRM was investigated following a modified procedure to that described by Chauvin et al. (2000). TRM gained during last step of the Thellier experiment (565 °C) was subsequently designated as TRM_1. At the same temperature, a new TRM (TRM_2) was given to all samples but using this time a long cooling time (~10 h). Finally, a third TRM (TRM_3) was created using the same cooling time (of about 45 min) as that used to create TRM_1. The effect of CR upon TRM intensity was estimated by calculating percent variation between the intensity acquired during a short and a long cooling time (TRM_1 and TRM_2). Changes in TRM acquisition capacity were estimated by means of the percent variation between the intensity acquired during same cooling time (TRM_1 and TRM_3).

TRM anisotropy corrections can be implemented in various ways (e.g., McCabe et al., 1985; Selkin et al., 2000; Chauvin et al., 2000, among others). It essentially requires the creation of a TRM along six mutually perpendicular directions (+*X*, +*Y*, +*Z*, −*X*, −*Y*, −*Z*) by cooling them from 600 °C to room temperature in a known magnetic field. This involves six additional heatings, which may significantly alter the magnetic mineralogy of the samples. To circumvent this time-consuming procedure, individual specimens (belonging to the same fragment) were embedded into the salt pellet in the six above-described positions. In this way, possible bias due to TRM anisotropy effects would be canceled, as attested by the results of our various previous test experiments (Morales et al., 2009).

AI data are reported on NRM–TRM plots (upper and lower left side of Fig. 7) and results are given in Table 2. NRM–TRM plot with the TRM normalized by the maximum TRM were used for clarity. We accepted determinations that meet the following criteria: (1) determination obtained from at least 4 NRM–TRM points corresponding to a NRM fraction larger than 1/3, (2) quality factor (Coe et al., 1978) of 5 or more, and (3) positive 'pTRM' checks, i.e., the deviation of 'pTRM' checks were less than 15%. Directions of NRM remaining at each step obtained from the AI experiments are reasonably linear and point to the origin (right part of Fig. 7). No deviation of NRM remaining directions towards the direction of applied laboratory field was observed. Cooling rate correction was not applied when corresponding changes in TRM acquisition capacity were higher than 15% (Table 2). Accepted data are only those cooling rate corrected values having passed all above criteria (data in column '$H_{accepted}$'). Finally, 52 samples, coming from

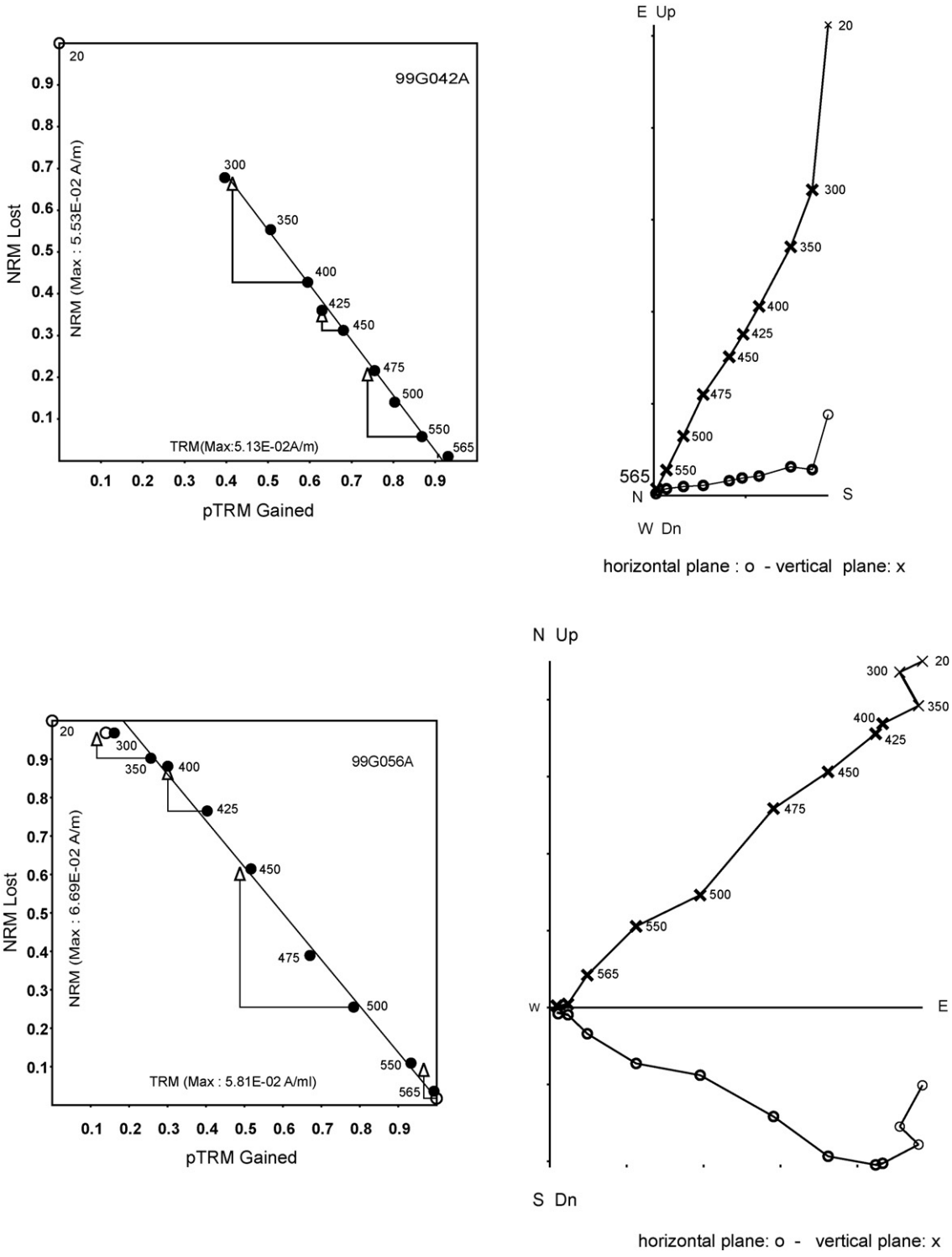

Fig. 7. Representative NRM–TRM plots and associates orthogonal vector demagnetization diagrams for the Kaminaljuyu samples. In the NRM–TRM plots, right angle arrows refer to the "pTRM" checks. On the orthogonal diagrams the numbers refer to the temperatures in °C. o—projection into the horizontal plane, x—projection into the vertical plane.

10 individual pottery fragments, yielded acceptable AI estimates (Table 3).

6. Main results and discussion

The mean archaeointensity values per pottery fragments range from (15.3 ± 2.8) to $(43.5 \pm 3.9)\,\mu T$ with a mean value of $(31.7 \pm 10.4)\,\mu T$, while corresponding Virtual Axial Dipole Moments (VADMs) range from $(3.6 \pm 0.7$ to $10.3 \pm 0.9) \times 10^{22}$ Am^2. This corresponds to a mean VADM value of $(7.5 \pm 2.5) \times 10^{22}$ Am^2, which is close to the present day field strength. These data were obtained according to strict – nowadays worldwide used – individual determinations acceptance criteria. For these samples the NRM fraction f used for determination ranges between 0.44 and 0.97 and the quality factor q from 7 to 26. So called 'pTRM checks' were also included in the methodology used.

Table 2
Summary of AI experiments: T_{min}–T_{max}, temperature range used for AI estimation H; n, number of NRM–TRM points used for the determination; H, ant: uncorrected H; sH, standard deviation of H; H ant crc, cooling rate corrected H; $H_{accepted}$, accepted H after CRC and acceptance criteria application; f, g and q: fraction of extrapolated NRM used for intensity determination, gap and quality factor (Coe et al., 1978), respectively. Represent samples exhibiting changes in TRM acquisition capacity higher than 15%. The laboratory field was set to 30 μT during the experiment.

Specimen	$T_{min-max}$ [°C]	n	$H_{ant\ UC}$ [μT]	σ $H_{ant\ UC}$ [μT]	$H_{ant\ CRC}$ [μT]	$H_{accepted}$ [μT]	f	g	q
99A011A	200–525	9	17.67	2.31			0.433	0.805	2.67
99A013A	200–500	7	19.38	1.80			0.352	0.807	3.07
99A014A	200–525	9	13.62	1.60			0.299	0.819	2.09
99A015A	200–525	9	22.46	3.19			0.398	0.824	2.31
99A018A	400–565	7	32.69	2.17	30.3	30.3	0.694	0.746	7.81
99A019A	400–565	7	54.72	2.54	50.7	50.7	0.667	0.513	7.38
Mean			26.8		27.2	40.5	0.47	0.75	4.2
s.d.			15.1		12.6	14.4	0.17	0.12	2.6
99A021A	300–565	8	54.69	5.30	51.6	51.6	0.839	0.807	6.99
99A023A	200–565	11	39.67	1.17	37.8	37.8	0.860	0.816	23.83
99A025A	300–565	9	40.36	4.96			0.798	0.853	5.54
99A026A	200–565	11	37.36	5.10			0.816	0.848	5.07
99A027A	200–565	11	34.40	2.19	33.6	33.6	0.844	0.844	11.17
99A028A	200–565	11	43.46	3.93	45.8	45.8	0.803	0.863	7.66
99A029A	200–565	11	44.94	1.45	42.3	42.3	0.839	0.823	21.35
Mean			42.1		42.4	42.2	0.83	0.84	11.7
s.d.			6.6		5.9	7.0	0.02	0.02	7.8
99A031A	200–565	11	50.33	2.85	38.0	38.0	0.856	0.844	12.76
99A032A	200–565	11	49.05	2.79	48.9	48.9	0.867	0.847	12.90
99A033A	200–565	11	50.22	2.99	47.8	47.8	0.857	0.840	12.08
99A034A		10	53.87	5.73	40.5	40.5	0.913	0.828	7.11
99A035A	20–565	12	50.59	1.37	43.4	43.4	0.925	0.893	30.55
99A036A	200–565	11	40.64	3.11	44.5	44.5	0.855	0.862	9.64
99A037A		10	48.39	4.30	41.7	41.7	0.843	0.863	8.18
Mean			49.0		43.5	43.5	0.87	0.85	13.32
s.d.			4.1		3.9	3.9	0.03	0.02	7.93
99A041A	20–565	12	35.34	2.99	34.3	34.3	0.967	0.876	10.00
99A042A	20–565	12	44.52	3.82	46.9	46.9	0.866	0.883	8.91
99A043A	20–565	12	44.00	3.28	48.4	48.4	0.953	0.885	11.32
99A044A	20–565	12	35.82	3.16	39.2	39.2	0.893	0.880	8.90
99A045A	20–565	12	42.69	2.94	41.4	41.4	0.989	0.871	12.53
99A046A	20–565	12	39.93	2.65	39.9	39.9	0.996	0.861	12.92
99A047A	20–565	12	38.56	2.94	42.9	42.9	0.924	0.886	10.75
99A048A	20–565	12	39.50	3.48			0.989	0.868	9.75
99A049A	20–565	12	33.92	2.62	37.7	37.7	0.890	0.886	10.20
Mean			39.4		40.8	41.3	0.94	0.88	10.6
s.d.			3.8		4.6	4.7	0.05	0.01	1.4
99A052A	200–565	11	39.90	1.08			0.721	0.833	22.13
99A056A	200–565	11	35.31	2.62		36.3	0.863	0.868	10.09
99A057A	250–65	10	32.78	2.28			0.612	0.856	7.53
99A058A	200–565	11	53.47	7.07			0.789	0.865	5.16
Mean			40.4		34.5	36.3	0.61	0.69	9.5
s.d.			9.2		6.7	2.6	0.33	0.38	7.5
99G061A	300–565	9	33.35	1.11	27.6	27.6	0.568	0.724	12.34
99G062A	300–565	10	37.65	0.63	30.8	30.8	0.559	0.866	29.07
99G063A	300-565	10	37.19	0.97	30.4	30.4	0.524	0.858	17.26
99G064A	300–565	10	31.98	1.45	25.3	25.3	0.552	0.857	10.41
99G067A	NR	7	33.83	1.08	27.3	27.3	0.440	0.799	10.98
99G068A	300–425	4	41.10	1.37	34.2		0.229	0.610	4.20
Mean			35.8		29.3	28.3	0.48	0.79	14.0
s.d.			3.4		3.2	2.3	0.13	0.10	8.5
99G071A	300–550	9	14.56	1.00	13.1	13.1	0.744	0.766	8.32
99G072A	300–550	9	18.41	0.71	17.3	17.3	0.752	0.781	15.18
99G073A	300–550	9	14.82	0.97	13.4	13.4	0.65	0.721	7.17
99G074A	300–550	9	16.56	0.57	15.9	15.9	0.758	0.761	16.76
99G075A	300–550	9	13.91	0.94	13.4	13.4	0.745	0.75	8.26
99G076A	300–550	g	21.69	1.28	20.6	20.6	0.754	0.753	9.60
99G078A	300-–550	9	15.05	1.17	13.7	13.7	0.739	0.767	7.30
Mean			16.4		15.3	15.3	0.73	0.76	10.4
s.d.			2.8		2.8	2.8	0.04	0.02	3.9
99G081A	300–575	11	25.62	0.94	24.6	24.6	0.739	0.859	17.29
99G083A	300–575	11	32.06	1.88	31.2	31.2	0.668	0.822	9.36
99G084A	20–575	12	20.69	0.26	19.2	19.2	0.954	0.883	67.95
99G085A	300–565	10	38.59	1.37	35.8	35.8	0.803	0.861	19.50
99G086A	300–565	10	32.78	1.40	31.0	31.0	0.795	0.856	15.97
99G087A	300–565	9	25.91	0.66	24.5	24.5	0.814	0.834	26.83
Mean			29.3		27.7	27.7	0.80	0.85	26.2

Table 2(*Continued*)

Specimen	$T_{min-max}$ [°C]	n	$H_{ant\ UC}$ [μT]	σ $H_{ant\ UC}$ [μT]	$H_{ant\ CRC}$ [μT]	$H_{accepted}$ [μT]	f	g	q
s.d.			6.4		6.0	6.0	0.09	0.02	21.2
99G091A	20–575	11	20.78	0.83	16.8	16.8	0.874	0.873	19.18
99G092A	300–500	8	24.03	0.91	19.9	19.9	0.684	0.864	15.57
99G093A	300–550	11	30.21	0.94	24.0	24.0	0.665	0.872	18.63
99G094A	300–575	11	17.27	0.71	14.3	14.3	0.671	0.878	14.28
99G095A	400–575	10	28.90	1.28	23.6	23.6	0.68	0.877	13.44
99G096A	300–575	11	23.68	0.43	19.7	19.7	0.711	0.885	34.86
Mean			24.1		19.7	19.7	0.71	0.87	19.3
s.d.			4.9		3.8	3.8	0.08	0.01	8.0
99G0101A	300–565	10	27.45	0.37	24.4	24.4	0.649	0.867	41.68
99G0102A	300–500	7	25.14	2.85	22.8	22.8	0.287	0.805	2.04
99G0103A	300–550	11	21.80	0.83	18.7	18.7	0.662	0.867	15.14
99G0104A	300–575	11	22.77	0.63	20.5	20.5	0.758	0.88	24.23
99G0105A	300–575	11	26.85	0.77	23.7	23.7	0.693	0.872	21.08
99G0106A	NR								
Mean			24.8		22.0	22.0	0.61	0.86	20.8
s.d.			2.5		2.4	2.4	0.19	0.03	14.4

H lab [μT] = 28.5; N = 12.

Table 3
Age vs. AI results. Specimen (Lab ID) to sample (field name) association, age, age uncertainty, intensity, intensity uncertainty, and average intensity (of samples with the same age, when possible).

Lab ID	Sample	~Age (B.C.)	σ Age	Intensity [μT]	σ Intensity [μT]	Avg. int. [μT]	σ Avg. int. [μT]	VADM [Am^2]
99A01XA	K-60A	−900	100	40.5	14.4			9.58E+22
99G07XA	K-62h	−800	100	15.3	2.8			3.62E+22
99A02XA	E-42g	−500	100	42.2	7.0			9.99E+22
99A03XA	KJM-3B161-3	−400	100	43.5	3.9			1.03E+23
99G06XA	D-275-2b	−200	100	28.3	2.3			6.70E+22
99G10XA	D-275-8b	−200	100	22.0	2.4	25.2	4.5	5.21 E+22
99A05XA	D-304h	−150	100	36.3	2.6			8.59E+22
99A04XA	A-P-G-Sy	−100	100	41.3	4.7			9.77E+22
99G08XA	D-254/4d	−100	100	27.7	6.0	29.6	10.9	6.55E+22
99G09XA	D-254/4d	−100	100	19.7	3.8			4.66E+22
			Mean = 31.7				Mean = 7.5E+22	
			1σ = 10.4				1σ = 2.5E+22	

So called pTRM tail checks are often incorporated during the measurements (Riisager et al., 2002) to detect the presence of multidomain magnetic grains. We prefer to avoid this procedures because of additional heatings required. We believe that the contributions of grains with multidomain magnetic structure should be detected before the Thellier experiments as part of effort to select suitable sample for paleointensity measurements.

Archaeointensity data obtained in the present study differ from those of ArcheoInt data compilation (Genevey et al., 2008, data reduced to the place of ceramic production), with the present data slightly lying lower than those reported in ArcheoInt database for the southwest part of North America (Fig. 8). It should be noted however that old Mesoamerican data (more than 76% within the period 1965–1975) might be systematically biased by the fact that neither strict acceptance criteria nor cooling rate and/or remanence anisotropy corrections were applied to most of these data (Morales et al., 2009; López-Téllez et al., 2008).

Donadini et al. (2009) produced a series of time-varying spherical harmonic models of the geomagnetic field for the last 3000 years based on a new compilation of lake sediment records and the GEOMAGIA50v2 online database. The overall number of data is increased 50%. The data coming from archaeological artifacts and lavas are involved to construct the ARCH3K curves. The new CALS3k.3 model uses all available measurements from sediments, lavas and archaeological structures and currently provides the best global representation of the 0–3 ka field. Many of Guatemalan data agree reasonably well with ARCH3K model prediction mainly at 900 B.C., 500 B.C. and 400 B.C. The archaeointensity obtained at about 800 B.C. is clear outlier and its geomagnetic significance should be confirmed by further studies. Here is important to mention that due to the high humidity of the region, conservation is not so good

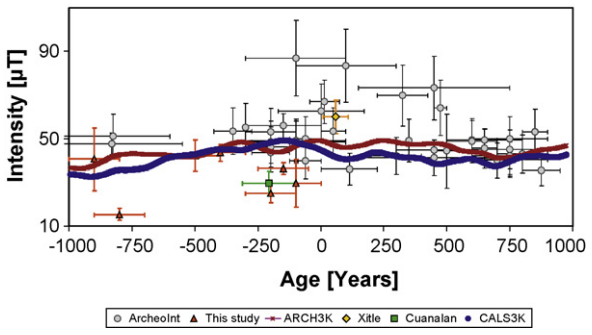

Fig. 8. Time variation of AI data (triangles) plotted together with ArcheoInt database (full circles; Genevey et al., 2008). Continuous brown (blue) line represents prediction from model ARCH3k (CALS3k), Donadini et al. (2009). Also shown Cuanalan (Rodriguez-Ceja et al., 2009, archaeological) and Xitle (Alva-Valdivia, 2005; Morales et al., 2007, volcanic) latest AI determination. (For interpretation of the references to color in the citation of this figure, the reader is referred to the web version of the article.)

resulting that the calculated ages are between more or less 100 years and in exceptional cases uncertainty is of 50 years. Relatively low values are observed between 300 B.C. and 0. However, our data agree well with currently available absolute intensity values from Mesoamerica (Rodriguez-Ceja et al., 2009) for the same time interval.

Acknowledgements

Pottery fragments from the Kaminaljuyú area were kindly donated from Dr. Hatch's collection. Financial support was provided by DGAPA research project IN-110308 and 'Proyecto Interno de Investigación G122'. We also acknowledge A. Gonzalez-Rangel for assistance with the experimental measurements and Dr. M. Rivas-Sanchez for help with microscopic observations. AG acknowledges the financial support given by CONACYT 54857. Comments and suggestions of reviewer (C. Constable) are especially appreciated, which greatly improved the manuscript.

References

Aitken, M.J., 1990. Science-based dating in archaeology, Longman Archaeology Series. Longman, 225–259.
Aitken, M.J., Pesonen, L.J., Leino, M., 1991. The Thellier paleointensity technique: minisamples versus standard size. J. Geomagn. Geoelectr. 43, 325–331.
Alva-Valdivia, L.M., 2005. Comprehensive paleomagnetic study on a succession of Holocene olivine-basalt flow: Xitle volcano (Mexico) revisited. Earth Planets Space 57, 839–853.
Bucha, V., Tylor, R.E., Berger, R., Haury, E.W., 1970. Geomagnetic intensity: changes during the past 3000 years in the western hemisphere. Science 168, 111–114.
Buddington, A.F., Lindsley, D.H., 1964. Iron–tatinium oxide minerals and synthetic equivalents. J. Petrol. 5, 310–357.
Coe, M.D., Flannery, K.V., 1967. Early Cultures and Human Ecology in South Coastal Guatemala. Smithsonian Press, Washington.
Coe, R.S., 1967. Paleo-intensities of the earth's magnétic field determined from tertiary and quaternary rocks. J. Geophys. Res. 72 (No. 12), 3247–3262.
Coe, R.S., Grommé, S., Mankinen, E.A., 1978. Geomagnetic paleointensities from radiocarbon-dated lava flows on Hawaii and the question of the pacific nondipole low. J. Geophys. Res. 83 (B4), 1740–1756.
Chauvin, A., Garcia, A., Lanos, Ph., Laubenheime, r.F., 2000. Paleointensity of the geomagnetic field recovered on archaeomagnetic sites from France. Phys. Earth Planet Inter. 120, 111–136.
Day, R., Fuller, M., Schmidt, V.A., 1977. Hysteresis properties of titanomagnetites: grain-size and compositional dependence. Phys. Earth Planet Inter. 13, 206–267.
Donadini, F., Korte, M., Constable, C.G., 2009. Geomagnetic field for 0–3 ka. 1. New data sets for global modeling. Geochem. Geophys. Geosyst. 10, Q06007, doi:10.1029/2008GC002295.
Draeger, U., Prevot, M., Poidras, T., Riisager, J., 2006. Single-domain chemical, thermochemical and thermal remanences in a basaltic rock. Geophys. J. Int. 106, 12–32.
Genevey, A., Gallet, Y., 2002. Intensity of the geomagnetic field in western Europe over the past 2000 years: new data from ancient French pottery. J. Geophys. Res. 107 (B11), 2285, doi:10.1029/2001JB000701.
Genevey, A., Gallet, Y., Constable, C.G., Korte, M., Hulot, G., 2008. ArcheoInt: an upgraded compilation of geomagnetic field intensity data for the past ten millennia and its application to the recovery of the past dipole moment. Geochem. Geophys. Geosyst. 9, Q04038, doi:10.1029/2007GC001881.
Haggerty, S.E., 1976. Oxidation of opaque mineral oxides in basalts. In: Rumble, D. (Ed.), Oxide Minerals (Short Course Notes). Mineral Soc. Am., vol. 3, pp. 1–100.
López-Téllez, J.M., Aguilar-Reyes, B., Morales, J., Goguitchaichvili, A., Calvo-Rathert M., Urrutia-Fucugauchi. J., 2008. Magnetic Characteristics and Archeointensity Determination on Some Mesoamerican pre-Columbian Potteries: Case Study of Quiahuiztlan Archeological Site (Veracruz, Gulf of Mexico, 900–1521 A.D.), Geofísica Internacional, 47 (4).
Lowe, G.W., 1977. The Mixe-Zoque as Competing Neighbors of the Early Lowland Maya. In: Adams, R.E.W. (Ed.), The Origins of Maya Civilization. University of New Mexico Press.
McCabe, C., Jackson, M., Ellwood, B., 1985. Magnetic anisotropy in the Trenton limestone: results of a new technique, anisotropy of anhysteric susceptibility. Geophys. Res. Lett. 12, 333–336.
Morales, J., Goguitchaichvili, A., Jaime Urrutia-Fucugauchi, 2007. Cooling rate effect as a cause of systematic overestimating of the absolute Thellier paleointensities: a cautionary note. Stud. Geophys. Geod. 51, 315–326.
Morales, J. Goguitchaichvili, A., Acosta, G., González-Morán, T., Alva-Valdivia, L., Robles-Camacho J., Hernández-Bernal, M., 2009. Magnetic properties and archeointensity determination on Pre-Columbian pottery from Chiapas, Mesoamerica. Earth Planets & Space. Special issue on "Magnetism of Volcanic Materials, Tribute to Works of Michel Prevot", doi:10.19EPS2364.10.29.
Nagata, T., Kobayashi, K., Schwarz, E.J., 1965. Archeomagnetic intensity studies of South and Central America. J. Geomagn. Geoelectr. 17, 399–405.
Popenoe de Hatch, M., 1997. Kaminaljuyú/San Jorge: Evidencia Arqueológica de Actividad Económica en el Valle de Guatemala, 300 a.C. a 450 d.C. Universidad del Valle de Guatemala, Guatemala.
Popenoe de Hatch, M., 2000. Kaminaljuyú Miraflores II: la naturaleza del cambio político al final del Preclásico. In: Laporte, J.P., Escobedo, H.L., de Suasnavar, A.C., Arroyo, B. (Eds.), X111 Simposio de Arqueología en Guatemala. Museo Nacional de Arqueología y Etnología, Guatemala, pp. 11–28.
Riisager, P., Riisager, J., Abrahamsen, N., Waagstein, R., 2002. Thellier paleointensity experiments on faroes flood basalts: technical aspects and geomagnetic implications. Phys. Earth Planet Inter. 131, 91–100.
Rodriguez-Ceja, M., Goguitchaichvili, A., Chauvin, A., Morales, J., Ostroumov, M., Manzanilla, L.R., Aguilar Reyes, B., Urrutia-Fucugauchi, J., 2009. An integrated magnetic and Raman spectroscopy study on some pre-Columbian potteries from cuanalan (a formative village in the valley of Teotihuacan) in Mesoamerica. J. Geophys. Res. 114, B04103, doi:10.1029/2008JB006106.
Selkin, P.A., Gee, J.S., Tauxe, L., Meurer, W.P., Newell, A.J., 2000. The effect of remanence anisotropy on paleointensity estimates: a case study from the Archean Stillwater complex. Earth Planet Sci. Lett. 183, 403–416.
Sinipoli, C.M., 1991. Aproaches to Archaeological Ceramics. Plenum Press, New York.
Tauxe, L., Mullender, T.A.T., Pick, T., 1996. Pot-bellies, wasp-waists and superparamagnetism in magnetic hysteresis. J. Geophys. Res. 95, 12337–12350.
Thellier, E., Thellier, O., 1959. Sur l'intensité du champ magnétique terrestre dans le passé historique et géologique. Ann. Géophysique. 15, 285–376.